Journal of Materials Chemistry C

Accepted Manuscript

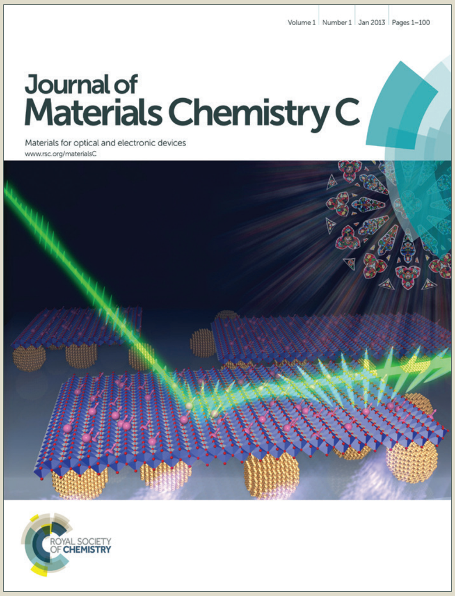

Journal Name RSCPublishing

COMMUNICATION

Cite this: DOI: 10.1039/x0xx00000x

Novel Design of remote phosphor ceramic plate for white generation in high power LEDs

Young Hyun Song,[a,∇] Gill Sang Han,[a,∇] Eun Kyung Ji,[e] Min-Ji Lee,[a] Ye Lim Song,[a] Dal Sung Kong,[b] Mong Kwon Jung,[c] Byung Woo Jeong,[d] Hyun Suk Jung [a*] and Dae-Ho Yoon[a,e*]

Received 00th January 2012,
Accepted 00th January 2012

DOI: 10.1039/x0xx00000x

www.rsc.org/

Here, we report a phosphor ceramic plate (PCP) made using $Y_3Al_5O_{12}$: Ce^{3+} (YAG:Ce) nanoparticles (NPs) with uniformly spherical size distribution for high-power light emitting diode (LED) applications. YAG:Ce NPs with diameters of 600 nm were synthesized by the forced hydrolysis method, and the typical excitation and emission of PCP made using YAG:Ce NPs was observed on blue emitting InGaN chips, as a conversion process for the generation of white LEDs with high luminous flux and thermal stability. In addition, for the improvement of the PCP characteristics, a novel design using graphene-embedded red phosphor layer (GRP) was utilized. The GRP-coated PCP displayed a higher CRI value of 82 and warm white light with a correlated colour temperature (CCT) of 3952 K compared to general PCP. This type of PCP is expected to be an outstanding candidate for the production of luminescence materials in various fields of optoelectronics.

White light emitting diode (WLEDs) technology has attracted customer attention due to considerable applications in the field of solid state lighting, as well as the accompanying advantages of compact size, low power consumption, long service time and environmental friendliness.[1-3] For the generation of white light, YAG:Ce phosphor is a very important component, including in the blue-emitting InGaN chip. However, YAG:Ce phosphor-based WLEDs have drawbacks related to thermal stress and low colour rendering index value due to the utilization of silicone resins with YAG:Ce phosphor and the limited spectral power distribution in the red spectral range under forward-bias current.[4, 5] This causes the correlated colour temperature (CCT) related to the white light to be unstable. The clear alternative to solve such problems is to use the GRP-coated PCP. Recently, instead of the utilization of YAG:Ce phosphor in silicone (PS) composite, PCPs known as remote phosphor (RP) have been used with InGaN blue chip for white light generation in high-power LEDs.[6] PCPs can easily be used with blue LED chips, in that the PCPs are placed far from the high-powered blue LED chip, which gives the PCPs excellent optical and thermal stability compared to the composite types. However, lower CCT (<4000 K) and CRI (>80) values are required for the illumination lighting.[7] The new challenge then becomes to further improve the illumination lighting source through application in white LEDs with high luminous flux, as well as by improving the characteristics of CCT and CRI. In this work, PCPs were fabricated using YAG:Ce NPs, after which GRP was coated on the PCP using a spin coater. Generally, PCPs are fabricated using bulk type YAG:Ce phosphor, which requires high temperature (>1700 °C) via vacuum sintering.[8] The approach used herein was to utilize YAG:Ce NPs synthesized by the forced hydrolysis method.[9] According to Roh et al., the YAG:Ce NPs fabricated using this method maintained their morphology and monodispersity after annealing.[10] To the best of our knowledge, the fabrication of PCPs with YAG:Ce NPs is a reasonable method. To satisfy low CCT and high CRI values, GRP was introduced on the PCPs at the same time to confer thermal stability. The rGO sheet is generally known to play the role of heat dissipation in LEDs.[11] In addition, graphene has attracted attention for its high transmittance and outstanding thermal and electric conductivity, as well as mechanical properties.[12, 13] In this work, the GRP and PCP were separately fabricated, as shown in Figure 1.

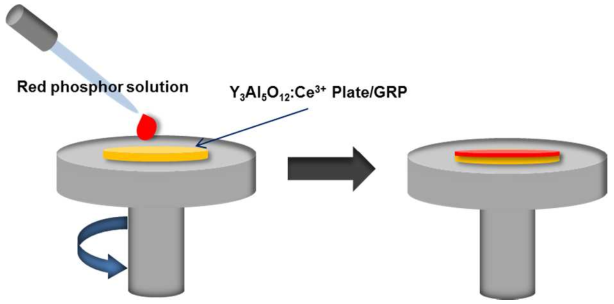

Figure 1. Illustration of GRP-coated PCP and White LED under operation.

The resulting GRP-coated PCP layered structure was then combined with a blue emitting LED chip to achieve the colour-stable warm white LEDs. YAG:Ce NPs were synthesized by the forced hydrolysis method. First, aluminum nitrate nonahydrate (Sigma-Aldrich, ≥98% pure), aluminum sulfate octadecahydrate (Sigma-Aldrich, ≥98% pure) and urea (Sigma-Aldrich, 99.5%) were used to produce 600 nm Al(OH)$_3$ particles. These materials were dissolved in deionized water and then aged at 98 ^{o}C for 4 h. The precipitate was then separated by centrifugation and washed several times. Second, yttrium nitrate (Sigma-Aldrich, 99.8%), cerium nitrate (Sigma-Aldrich, 99%), and urea (Sigma-Aldrich, 99.5%) were dissolved in deionized water. The synthesized Al(OH)$_3$ particles were homogeneously dispersed in the mixed solution, which was stirred vigorously at 98 ^{o}C for 3 h. The precipitate was isolated by centrifugation, washed with deionized water, and then dried using a lyophilizer. The resulting powder was annealed at 1200 ^{o}C for 4 h under a reducing atmosphere (5% H_2/95% N_2). The PCP was fabricated with YAG:Ce NPs, PVA and TEOS. These materials were mixed and milled with ZrO_2 balls for 24 h. The mixture was then packed into disks and sintered at 1600 ^{o}C for 24 h under a reducing atmosphere (5% H_2/95%N_2). The PCP obtained was then polished to the thickness of 100 μm. GRP was synthesized as per our previous study, with the modification that $Sr_2Si_5N_8$: Eu^{2+} red phosphor was employed. The final product was obtained through spin coating with the GRP of the thickness of 100 μm onto the PCP. The morphology was characterized using field-emission scanning electron microscopy (FE-SEM, JSM-7600F, JEOL). To observe the phase evolution, Power XRD (XRD, D-MAX 2500, Rigaku) measurements were carried out with the CuKα target being 20° ≤ 2θ ≤ 80°. The photoluminescence properties of the YAG:Ce NPs were measured by a room-temperature photoluminescence spectrometer (PL, PSI Co., Ltd./Korea) equipped with a 500 W Xenon discharge lamp. Raman spectroscopy (Renishaw spectrometer, 2.41 eV, and wave length, 514 nm) was also employed for analysis of the electronic structure of rGO. The EL and luminous flux of the final product under a 450 nm blue LED chip (IWS-S5552-UB-K1, ITSWELL, Korea) was measured as a function of input current and temperature with an Instrument Systems CAS-140CT.

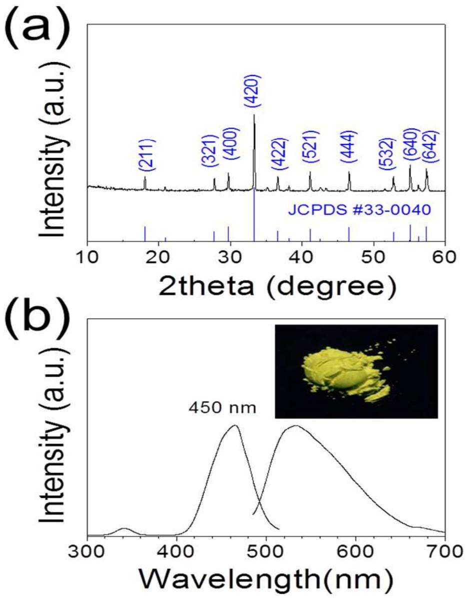

Figure 2. (a) XRD patterns of YAG:Ce NPs. (b) Excitation and emission spectra of YAG:Ce NPs. The inset shows an SEM image and photograph of YAG:Ce NPs

Figure 2 (a) shows the XRD patterns of the YAG:Ce NPs fabricated by the forced hydrolysis method. All diffraction peaks of the prepared YAG:Ce NPs were perfectly matched to the pure $Y_3Al_5O_{12}$ (YAG) phase, following JCPDS 33-0040. The Ce^{3+} ions, as an activator, were incorporated into the YAG structure without altering the charge of the original structure. Also, the SEM image of PCP is shown in figure S1(ESI†). The photoluminescence excitation and emission characteristics of the YAG:Ce NPs are shown in Figure 2(b). The two excitation bands of YAG:Ce NPs corresponded to the crystal field splitting band of the excited 5d state of the Ce^{3+} ions.[14] In addition, the emission spectrum originated from the transition from the 5d state to the 4f state.[15]

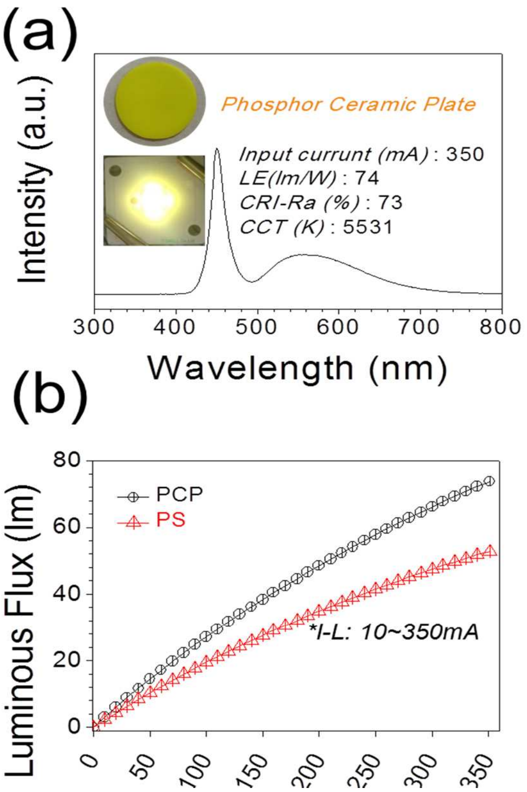

Figure 3. (a) EL spectra of PCP using YAG: Ce NPs. The inset shows the PCP and operation of the White LED. (b) I-L spectra of the PCP compared with PS.

Figure 3(a) shows the EL spectra of the white LED stacked PCP made using YAG:Ce NPs on a blue LED chip (λ=450 nm , P_{opt}=1 W). Under a current of 350 mA, the CRI value was 73, while the luminous efficacy was 74 lm/W. The input current-luminous flux (I-L) was analyzed with increase of the current from 10 to 350 mA, as shown in Figure 3(b). The luminous flux increased without any saturation effect since the blue light was converted into yellow light, to which the human eye is more sensitive.[16] PCP displayed higher luminous flux than the PS type with increase of the current from 10 to 350 mA because of the outstanding physical, chemical, and thermal stability of graphene, unlike the PS type, as well as the common design of the PCP to be packaged far from the blue LED chips.[11]

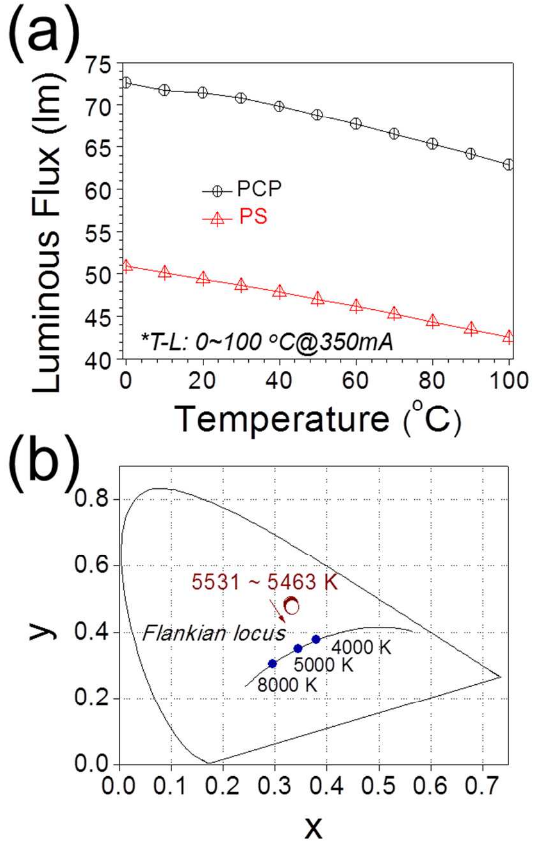

Figure 4. (a) T-L spectra of the PCP compared with PS. (b) CIE colour coordinates of PCP on blue LEDs

Temperature-luminous flux (T-L: 0~100 °C@350 mA) was analyzed to study the thermal and colour stability. Figure 4(a) shows the T-L properties of the PCP on blue LEDs (λ=450 nm , P_{opt}=1 W) compared with the PS type. It can be direct evidence for thermal conductivity. A decrease of the luminous flux was observed with increasing temperature under 350 mA. The PCP displayed that luminous flux was 64 lm at 100 ^{o}C; however, the blue LEDs with PS showed a lower value of the luminous flux of 43 lm when the temperature of device was at 100 ^{o}C. Figure 4(b) shows the CIE colour coordinates. The PCP displayed CCT variation from 5531 ~ 5463 K. Table S1(ESI†) summarizes the CCT variation of PCP compared to PS type. Overall, the PCP demonstrated better colour stability than PS on blue LED.

Raman spectroscopy analysis was next carried out on the developed materials. In order to realize warm–white LEDs with better thermal conductivity compared with the conventional remote phosphor, GRP was applied to the surface of the PCP using the spin-coating method. Figure 5 shows the Raman spectroscopy of rGO by the Hummers method. Raman spectroscopy is a well-known major technology used to provide an understanding of the bonding nature of carbon materials and to study the nature of the sp2 domain.[17] The G peak (1595 cm^{-1}), corresponding to the sp2 hybridized carbon, shifted towards lower wave number compared to that of GO, which agrees with previous reports. The D peak (1346 cm^{-1}) originated from the disorder-activated Raman mode. Both the G and D peaks arise from vibrations of sp^{2}-hybridized carbon atoms.[18]

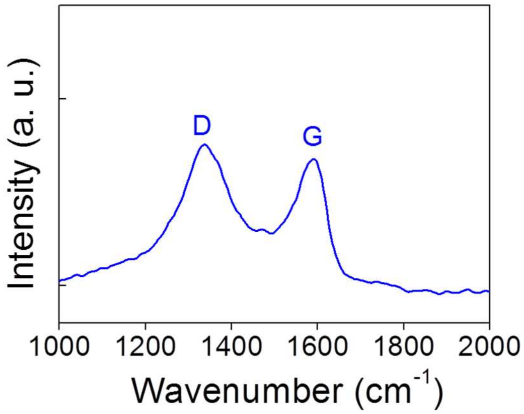

Figure 5. Raman spectrum of rGO.

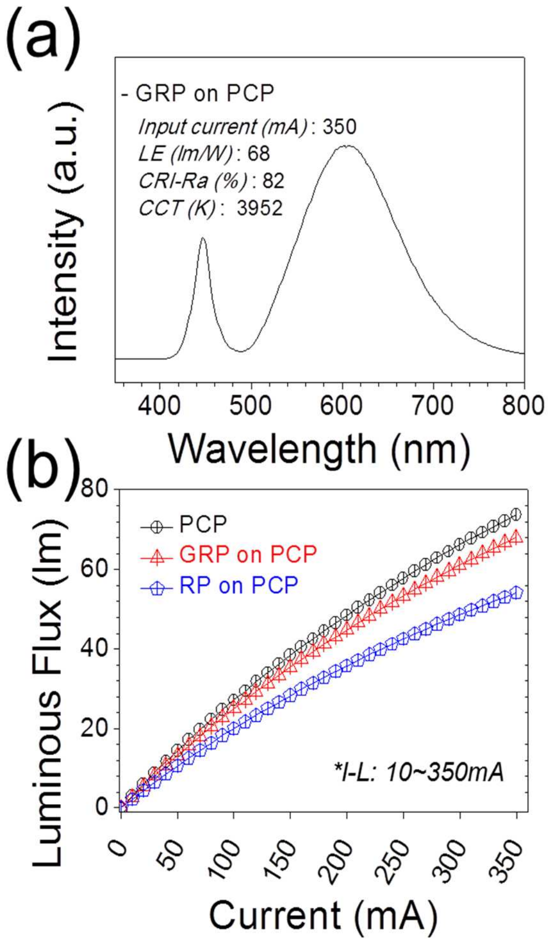

Figure 6. (a) EL spectrum of the fabricated samples. (b) I-L spectra of the fabricated samples

Figure 6(a) presents the EL spectrum of the GRP-coated PCP. Under the input current of 350 mA, the CRI of 82 and luminous efficacy of 68 lm/W were observed, while the CCT was 3952 K for the generation of warm-white light. In addition, the wavelength was shifted to the red region compared with PCP. The GRP-coated PCP displayed higher CRI and lower CCT values than PCP, satisfying conditions for the generation of warm-white light. I-L was increased as a function of the current, as shown in figure 6(b). The PCP showed higher luminous flux compared with GRP-coated PCP. This was attributed to the GRP, which was fabricated using polydimethylsiloxane (PDMS) materials. The PDMS materials were based on the polymer type. This type is very weak to heat generation by scattered light in LEDs. However, the GRP-coated PCP displayed higher luminous flux than RP-coated PCP because GRP contains rGO, which can show good thermal conductivity.

Figure 7(a) indicates the T-L properties of the fabricated sample on blue LED chips (λ=450 nm , P_{opt}=1 W). With increasing temperature, a drop in the luminous flux was observed due to heat generation of the device. Compared to the RP-coated PCP, GRP-coated PCP showed higher luminous flux due to the chemical and physical properties of rGO, including high thermal conductivity. The GRP-coated PCPs for application in white LEDs were analyzed with CIE colour coordinates, as shown in figure 7(b). The CCT variation of 3879 ~ 3952 K was observed compared with PCP. Based on these results, although the luminous flux of GRP-coated PCP was lower than PCP, it was concluded that the CCT of the white LEDs can be more stable than general type for the generation of warm white light, which proved their practical feasibility as colour down converters for applications in high-power LEDs.

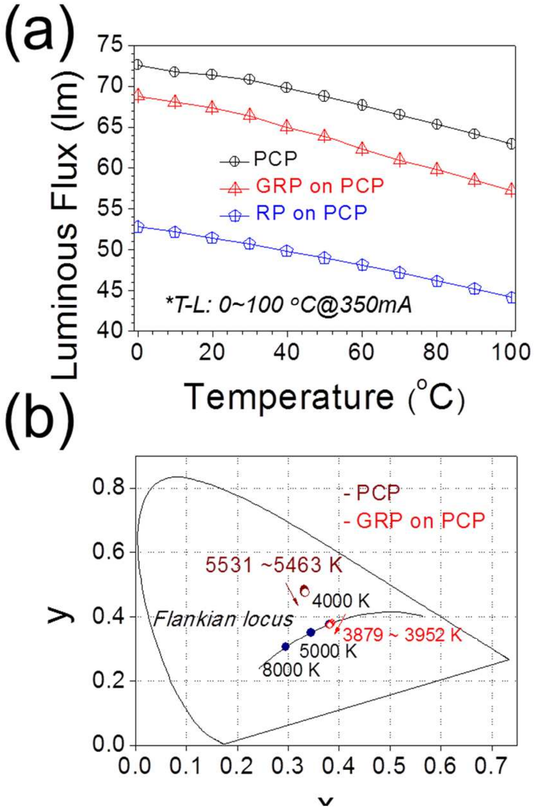

Figure 7. (a) T-L spectra of GPL on PCP. (b) CIE colour coordinates of PCPs on blue LEDs.

In the current study, we successfully fabricated GRP-coated PCPs to improve the chromaticity for applications in high-powered LEDs. Based on the power XRD and photoluminescence properties, the YAG:Ce NPs were perfectly synthesized for fabrication of the PCP. When GRP was applied on the PCP, higher CRI (82) and lower CCT (3952 K) values were observed than for the PCP alone. We hope that the use of GRP-coated PCP will be a very easy method for application in high-powered LEDs, wither higher feasibility compared with conventional remote phosphor because of the introduction of rGO. We suggest that this concept may be the next generation of remote phosphor, as a candidate for the generation warm white LEDs, as well as high-powered LEDs.

This research was supported by the Basic Science Research Program through the National Research Foundation of Korea (NRF), funded by the Ministry of Education (NRF-2013R1A1A2059280). This work was also supported by National Research Foundation of Korea (NRF) grants funded by the Ministry of Science, ICT & Future Planning (MSIP) of Korea under contract no. NRF-2014R1A2A2A01007722.

Notes and references

[a] School of Advanced Materials Science & Engineering, Sungkyunkwan University, Suwon 440-746, Republic of Korea. Email: dhyoon@skku.edu, hsjung1@skku.edu

[b] Department of Energy Science, Sungkyunkwan University, Suwon 440-746, Republic of Korea

[c] Hyosung Corporation, R&D Business Labs, Anyang 431-080, Republic of Korea

[d] LG Electronics, Future Device R&D Department, Seoul 137-724, Korea

[e] SKKU Advanced Institute of Nanotechnology (SAINT), Sungkyunkwan University, Suwon 440-746, Republic of Korea

[▿] These authors contributed equally to this work.

† Electronic supplementary information (ESI) available: The SEM images of (a) YAG: Ce NPs, (b) The fabricated PCP using YAG: Ce NPs; The comparison of CCT variation with PCP and PS.

1. Lee, Y. K.; Kim, Y. H.; Heo, J.; Im, W. B.; Chung, W. J Opt. Lett. 2014, 39, 4084.
2. Lee, J. S; Unithrattil, S.; Kim, S.H.; Lee, I. J.; Lee, H. G.; Im, W. B. Opt. Lett. 2013, 38, 3298.
3. Feezell, D. F; Speck, J.S.; DenBaars, S.P.; Nakamura, S. J. Display Tech. 2013, 9, 190.
4. Kim, J. S.; Yang, S. C.; Bae, B. S. Chem. Mater. 2010, 22, 3549.
5. Judd, D. B. J. Opt. Am. 1964, 54, 1031.
6. Sheu, J. K.; Chang, S. J.; Kuo, C. H.; Su, Y. K.; Wu, W. L.; Lin, Y. C.; Lai, W. C.; Tsai, J. M.; Chi, G. C.; Wu, R. K. IEEE Photonic Tech. L. 2003, 15, 18.
7. Georghiades, A.S.; Belhumeur, P.N.; Kriegman, D. J. IEEE T. Pattern Anal. 2001, 23, 643.
8. Roushan, M.; Zhang, X.; Li, J. Angew. Chem. 2012, 124, 451.
9. Hassanzadeh-Tabrizi, S.A.; Taheri-Nassaj, E.; Sarpoolaky, H. J. Alloy Compd. 2008, 456, 282.

10. Roh, H. S.; Kim, D. H.; Park, I. J.; Song, H. J.; Hur, S. Y.; Kim, D. W.; Hong, K. S. J. Mater. Chem. 2012, 22, 12275.
11. Song, Y. H.; Han, G. S.; Mang, S. R.; Jung, M. K.; Jung, H. S.; Yoon, D. H. J. Mater. Chem. C, 2015, 3, 235.
12. Sun, P.; Zhu, M.; Wang, K.; Zhong, M.; Wei, J.; Wu, D.; Zhu, H. Appl. Mater. Interfaces, 2013, 5, 9563.
13. Malekpour, H.; Chang, K. H.; Chen, J. C.; Lu, C. Y.; Nika, D. L.; Novoselov, K. S.; Balandin, A. A. Nano Lett. 2014, 14, 5155.
14. Robbins, D. J. J. Electrochem. Soc. 1979, 126, 1550.
15. Jacobs, R. R.; Krupke, W. F.; Weber, M. J. Appl. Phys. Lett. 1978, 33, 410.
16. Garcia, J. M.; Dalla-Costa, A.; Cardesin, J.; Alonso, J. M.; Rico-Secades, M. IEEE T. Power Electr. 2009, 24, 1107.
17. Coffman, F. L.; Cao, R.; Pianetta, P. A.; Kapoor, S.; Kelly, M.; Terminello, L. J. Appl. Phys. Lett. 1996, 69, 568.
18. Kochmann, S.; Hirsch, T.; Wolfbeis, O.S. J. Fluoresc. 2012, 22, 849.